

This is the preprint of the paper that will appear in
conference proceedings of Artificial Intelligence in
Healthcare (AiiH) 2025

GNN’s Uncertainty Quantification using Self-Distillation

Hirad Daneshvar¹*[0000–0002–6210–9306] and Reza Samavi^{1,2}[0000–0001–6768–0168]

¹ Toronto Metropolitan University, Toronto, ON, Canada
{hirad.daneshvar,samavi}@torontomu.ca

² Vector Institute, Toronto, ON, Canada

Abstract. Graph Neural Networks (GNNs) have shown remarkable performance in the healthcare domain. However, what remained challenging is quantifying the predictive uncertainty of GNNs, which is an important aspect of trustworthiness in clinical settings. While Bayesian and ensemble methods can be used to quantify uncertainty, they are computationally expensive. Additionally, the disagreement metric used by ensemble methods to compute uncertainty cannot capture the diversity of models in an ensemble network. In this paper, we propose a novel method, based on knowledge distillation, to quantify GNNs’ uncertainty more efficiently and with higher precision. We apply self-distillation, where the same network serves as both the teacher and student models, thereby avoiding the need to train several networks independently. To ensure the impact of self-distillation, we develop an uncertainty metric that captures the diverse nature of the network by assigning different weights to each GNN classifier. We experimentally evaluate the precision, performance, and ability of our approach in distinguishing out-of-distribution data on two graph datasets: MIMIC-IV and Enzymes. The evaluation results demonstrate that the proposed method can effectively capture the predictive uncertainty of the model while having performance similar to that of the MC Dropout and ensemble methods. The code is publicly available at https://github.com/tailabTMU/UQ_GNN.

Keywords: Uncertainty Quantification · Graph Neural Network · Medical AI · Trustworthy Machine Learning

1 Introduction

The use of Graph Neural Networks (GNNs) has seen an increase in the medical domain for tasks including diagnosis [17], medication recommendation [21], disease prediction, and readmission and mortality prediction [27,4]. To effectively

use GNNs in healthcare, clinicians need to trust the model predictions [3]. Quantifying the predictive uncertainty of GNNs is crucial for building users’ confidence in predictions of the models, especially in sensitive areas like healthcare [23].

Bayesian methods provide precise uncertainty quantification in neural networks but are computationally expensive. Alternatively, ensemble methods quantify uncertainty by measuring disagreement among multiple single network predictions and the ensemble outcome as the reference [16]. To ensure diversity in the ensemble, knowledge distillation is employed, where a teacher model is first trained and then its predictions are used to guide the training of smaller student models [25]. Despite the improved scalability, the ensemble approach remains computationally expensive, particularly with deep GNNs, as several deep individual networks need to be trained. Furthermore, the disagreement metric can be imprecise when the ensemble contains diverse models. The following example further illustrates the limitations of the disagreement metric.

Consider a clinical institute that employs three GNN classifiers, C1, C2 (deeper than C1), and C3 (deeper than C2), to diagnose Common Cold, COVID-19, and Influenza. Predictions from C3 serve as the reference. C1 and C2 are used to assess the uncertainty of predictions. If all models agree on COVID-19 (Patient 1), uncertainty is low; when C1 and C2 predict COVID-19 but C3 predicts Influenza (Patient 2), uncertainty should be higher. However, the disagreement metric assigns the same uncertainty (0.070) to both cases (Table 1), demonstrating the lack of expressivity of the current disagreement metric.

Table 1. Disagreement and classification by three GNNs (with increasing depth from C1 to C3) for two patients, highlighting the disagreement metric’s limited informativeness when shallower GNNs (C1 and C2) deviate from the Reference GNN (C3).

Patients	Model	Common Cold	Covid-19	Influenza	Disagreement
Patient 1	C1	0.3	<i>0.38</i>	0.32	0.070
	C2	0.3	<i>0.4</i>	0.3	
	C3	0.2	<i>0.5</i>	0.3	
Patient 2	C1	0.301	<i>0.414</i>	0.286	0.070
	C2	0.301	<i>0.442</i>	0.257	
	C3	0.3	0.32	<i>0.38</i>	

In this paper, we propose a self-distillation-based approach for efficient and precise uncertainty quantification of GNNs. Self-distillation represents a particular kind of knowledge distillation where the teacher and student models are part of a single model [24]. Efficiency is achieved through deepest classifier teacher distillation in a multi-classifier GNN. During training, the shallower classifiers learn from the deepest classifier using a combined cross-entropy and Kullback–Leibler (KL) divergence loss. The precision is improved by a weighted disagreement metric that emphasizes the diversity of the classifiers. The metric assigns higher weights to deeper classifiers when their predictions diverge from those of the teacher. Since deeper classifiers utilize richer representations, a discrepancy between the teacher and deeper classifiers for classifying a data point indicates that

the classifier is having difficulty aligning itself with the teacher (i.e., the deepest) classifier, causing the data point to be considered as a hard example [24].

The key contributions of this paper are as follows. First, we develop a self-distillation-based method for uncertainty quantification that is more efficient than training separate individual GNNs in an ensemble. Second, we propose a refined uncertainty metric that demonstrates greater precision by incorporating diversity among individual networks of an ensemble. Finally, we experimentally demonstrate the efficiency of our approach in quantifying GNN uncertainty.

2 Related Work

MC Dropout [15] and last-layer dropout [1] have been applied to GNNs for Bayesian inference, learning parameter distributions and quantifying uncertainty through the variance of multiple predictions. A Bayesian semi-supervised Graph Convolution Neural network [26] uses predictive variance for uncertainty, particularly in low-data scenarios. Bayesian methods are computationally expensive and require multiple predictions for uncertainty estimation. The proposed approach aims to achieve efficient uncertainty quantification in any GNN classifier.

Conformal prediction is a statistical framework that produces prediction intervals for a pretrained model with a guarantee on the prediction’s reliability [22]. Although integrating conformal interval predictions into distributional methods of uncertainty quantification is challenging, probabilistic methods have been developed to provide certified boundaries of computed uncertainty [13,14]. Conformalized GNN (CGNN) extends conformal prediction to GNNs for uncertainty quantification [11], by using the output of a GNN to train a second GNN for conformal corrections and finally applying standard conformal prediction to generate prediction sets. Another approach applies conformal prediction directly to pre-trained GNNs using a graph-aware conformity score based on neighbourhood diffusion [8]. These methods primarily focus on node classification, requiring modifications for graph classification. Our proposed approach can be applied to any classification task using GNNs, including node and graph classification.

Ensembles can be utilized to quantify model uncertainty by aggregating predictions from multiple models. [16] proposed a general deep ensemble framework to quantify model uncertainty by using the KL divergence of the individual network predictions in the ensemble, and the ensemble outcome. [1] trained independent GNNs and used the variance of their predictions as an uncertainty measure. The previous approaches mainly focused on training identical networks in an ensemble. Teacher-student knowledge distillation has been utilized to add diversity to the ensemble [25]. [6] utilized a GNN with a multi-head classification layer, in which the classification heads utilize the same GNN backbone, and used the variance of prediction to estimate uncertainty. However, training an ensemble is computationally expensive, and existing disagreement metrics may not be suitable for diverse ensembles. Our approach trains classifiers simultaneously with an uncertainty metric that captures the diversity of the models.

3 Self-Distillation for Uncertainty Estimation

In this section, we will first provide the necessary setup for knowledge distillation and self-distillation. We then present the training phase of the method and the proposed uncertainty quantification metric. We utilize GNNs for the graph classification task throughout this work, even though the approach is generalizable to any GNN’s classification task, including graph and node classification.

3.1 Problem Setup

Knowledge Distillation is an effective technique for training a smaller, simpler student model by learning from a larger, more complex teacher model, achieving performance comparable to that of the teacher model while having reduced computational demands. The approach facilitates the deployment of neural networks on resource-constrained devices [10,7]. Traditional knowledge distillation starts by training a teacher model. Subsequently, the teacher’s soft output probabilities (soft labels) are used to train one or more separate, typically shallower, student models that aim to replicate the teacher’s behavior [20]. This process effectively transfers knowledge from the teacher to the student. However, the training process can be resource-intensive, requiring the separate training of both the teacher and potentially multiple student models.

Self-Distillation is a specific type of knowledge distillation [7] that uses the same network as both the teacher and the student and offers a solution for the challenges of knowledge distillation in over-parameterized GNNs [2]. In contrast to traditional knowledge distillation, self-distillation involves transferring knowledge from the model’s deeper layers to its shallower ones [24,7]. In self-distillation, a classifier is placed after each hidden layer, where the classifier connected to the deepest layer acts as a teacher. For example, a GNN with three hidden layers would have three classifiers, each using the output of its previous layers for classification. Consequently, deeper classifiers utilize more comprehensive representations of the input, having access to features extracted by deeper layers. When hidden layers have different output dimensions, a harmonization layer is applied before all classifiers, except the deepest one. This layer, often a fully connected layer, adjusts the output shape of its preceding hidden layer to match the final hidden layer, ensuring uniform input shapes for all classifiers.

3.2 Training with Self-Distillation

Figure 1 shows a sample neural network with three hidden layers and three classifiers developed for self-distillation. Let $f : \mathcal{G} \rightarrow \mathcal{Y}$ be a GNN classifier trained on $D = \left\{ (G_i, y_i) \mid G_i \in \mathcal{G}, y_i \in \mathcal{Y} \right\}_i^N$. The network f consists of m hidden layers, i.e., hidden graph operators, each followed by a classifier c_l , such as a Multilayer Perceptron (MLP), where $1 \leq l \leq m$. Each hidden layer is a feature extractor $h_l(G)$ that uses the node features and the adjacency matrix of a graph

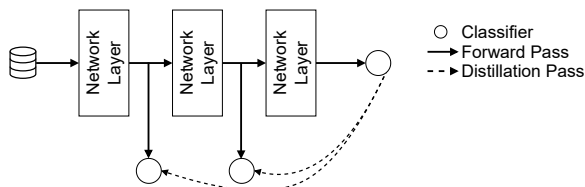


Fig. 1. A network structure with 3 layers and 3 classifiers used in self-distillation.

G to extract graph features. $c_l(h_l(x_i))$ represents the predicted output of the classifier using the extracted features at layer l .

During the training process, each classifier learns to mimic the teacher model, i.e., the deepest classifier in Figure 1. To this end, a total distillation loss function is used. The total distillation loss is based on the work by [24] and has two components: *distillation loss* and *feature penalty*. The distillation loss minimizes the compound cross-entropy loss and KL divergence loss of every classifier, and the feature penalty minimizes a penalty for features extracted by shallower models. The training objective is to minimize the total distillation loss.

Definition 1. For each graph G_i , the distillation loss L_{dis}^i is the mean of layer-wise weighted sums of two components: the cross-entropy of the classifier output at layer l , $c_l(G_i)$, with the true label, and the KL-divergence between the student’s soft labels at layer l , q_l^i , and the teacher’s soft labels, q_t^i . The loss is computed as

$$L_{\text{dis}}^i = \frac{1}{m} \sum_{l=1}^m \left((1 - \alpha_l) L_{\text{CE}_l}^i + \alpha_l L_{\text{KL}_l}^i \right), \quad (1)$$

where $\alpha_l \in [0, 1]$ is the imitation parameter for each classifier. The L_{CE_l} and L_{KL_l} are the cross-entropy and KL divergence loss for layer l , respectively. The imitation parameter of the teacher model is set to zero. As a result, the teacher model will be trained only using the cross-entropy loss.

The cross-entropy loss of the model is formulated as

$$L_{\text{CE}_l}^i = - \sum_{c=1}^k y_i^c \log(q_l^i), \quad (2)$$

and the KL divergence loss is formulated as

$$L_{\text{KL}_l}^i = \sum_{c=1}^k q_l^i \log\left(\frac{q_l^i}{q_t^i}\right). \quad (3)$$

Similar to [24], we add a penalty for features extracted by shallower models.

Definition 2. For each graph G_i , the penalty L_{pen}^i is the weighted average of the squared ℓ_2 -norm of the features extracted in each layer, h_l , and the features extracted by the teacher model, h_t . The penalty is computed as

$$L_{\text{pen}}^i = \frac{1}{m} \sum_{l=1}^m \lambda_l L_2(h_l^i, h_t^i), \quad (4)$$

where $\lambda_l > 0$ is the trade-off parameter for each classifier and L_2 is the squared ℓ_2 -norm loss. The λ_l parameter for the teacher model is set to zero.

The total distillation loss for all n graphs in the training dataset is the mean of the combination of both the distillation loss and penalty component, which is

$$L = \frac{1}{n} \sum_{i=1}^n L_{\text{dist}}^i + L_{\text{pen}}^i. \quad (5)$$

3.3 Uncertainty Quantification

To quantify uncertainty, we utilize the difference between predictions of each classifier c_l , where $1 \leq l \leq m-1$, and the teacher classifier c_t , where $t = m$. Our intuition of uncertainty quantification is rooted in the disagreement metric used to quantify uncertainty in a deep ensemble [16]. This notion can be formally defined as a disagreement between the probability predictions of each individual model and that of the ensemble. In other words, in a deep ensemble, if the prediction of each model aligns with the prediction of the ensemble, there would be less prediction uncertainty for the given data.

Definition 3. The disagreement metric for a graph G in an ensemble of m GNNs is the sum of KL divergences between each model’s prediction and the ensemble’s outcome, which is,

$$\text{disagreement} = \sum_{l=1}^m KL(P_l || P_{\text{outcome}}), \quad (6)$$

where P_{outcome} is the prediction probabilities of the ensemble model.

The KL-divergence measures the difference between two probability distributions. When the distribution of both probabilities is the same, the KL-divergence is zero, and the value gets unboundedly larger as the two probability distributions diverge. KL-divergence can be computed as

$$KL(P_l(y|G) || P_{\text{outcome}}(y|G)) = \sum_{c=1}^k P_l(y_c|G) \log \left(\frac{P_l(y_c|G)}{P_{\text{outcome}}(y_c|G)} \right), \quad (7)$$

where k is the total number of labels.

In self-distillation, every layer is followed by a shallow classifier (e.g., a two-layer MLP), where the preceding layers and the classifier are considered as a student model, except for the deepest layer, which acts as the teacher. Deeper classifiers utilize richer representations. Therefore, if the predictions of a shallow classifier deviate from those of deeper classifiers, the instance can be considered as a hard example [24]. This distinction arises because deeper classifiers exploit more informative feature representations. The disagreement metric (Equation 6), as shown in Table 1, treats all models equally, especially when predicted classes differ from the outcome of the deepest network, i.e. the reference/teacher model. To capture the impact of network depth diversity in such disagreements, we propose a weight function to differentiate varying depths of the models.

Weight Function. The weight function puts more emphasis on deeper student classifiers when their prediction disagrees with the outcome, thus increasing the impact of their disagreement on the uncertainty value. This function, $W(d)$, is monotonically increasing with depth ($W(1) < W(2) < \dots < W(L)$) and bounded between 1 and 2. If a student’s prediction matches the outcome, its weight is 1; otherwise, the weight increases with its depth. We use the teacher’s prediction as the outcome since all shallower classifiers mimic the teacher model.

The uncertainty of the model for a graph G can be formally quantified as

$$disagreement_w = \sum_{l=1}^m W(l) \times KL(P_l || P_{teacher}), \quad (8)$$

where W is a weight function and $P_{teacher}$ is the predicted probabilities of the teacher model. The weight function assigns higher weights to classifiers based on their depth relative to the deepest classifier. Specifically, classifiers with feature extractors of greater depth receive higher weights. The weight of a classifier at layer l can be computed by

$$W_{lin}(l) = 1 + \frac{L - D(l)}{L} \mathbb{1}_{\{y_l \neq y_{teacher}\}}, \quad (9)$$

where L is the total number of layers in the network, $D(i)$ is the distance of the classifier i from the deepest layer and $\mathbb{1}$ is the indicator function, which returns one if the given condition (e.g., if y_l differs from $y_{teacher}$) is met; otherwise, it returns zero. y_l and $y_{teacher}$ are the predicted class by the l th classifier and the predicted class by the teacher classifier, respectively.

Alternatively, the weight function can be nonlinear. However, the impact of using a nonlinear function needs further investigation. To show the potential of utilizing a nonlinear weight function, we introduce a nonlinear alternative $1 \leq W_{nonlinear}(l) \leq 2$ that assigns higher weights compared to $W_{linear}(l)$. The nonlinear weight function is

$$W_{nonlin}(l) = (-\exp(D(l) - L) + 2) \mathbb{1}_{\{y_l \neq y_{teacher}\}}, \quad (10)$$

where the \exp component exponentially amplifies the disagreement effect in deeper layers. Mathematically, both $W_{lin}(l)$ and $W_{nonlin}(l)$ weight functions

are sound as they are monotonically increasing. The choice between linear or non-linear weight functions can be considered as a domain-specific parameter to make the uncertainty quantification more or less conservative. Nevertheless, understanding the impact requires further empirical investigation.

Weighted disagreement (Equation 8) uses unbounded KL Divergence, which increases significantly with larger differences between $P_{outcome}$ and P_l , especially near zero probabilities in $P_{outcome}$. To address this, we use bounded Jensen-Shannon Divergence ($0 \leq JSD \leq \log_b(2)$), which is based on KL Divergence. Thus, our proposed uncertainty metric can be computed as

$$UC = \sum_{l=1}^m W(l) \times JSD(P_l || P_{teacher}), \quad (11)$$

where the JSD can be computed by

$$JSD(P_l || P_{outcome}) = \frac{1}{2} \left(KL(P_l || M) + KL(P_{outcome} || M) \right), \quad (12)$$

where M is a mixture distribution of P_l and $P_{outcome}$ and can be computed as $M = \frac{1}{2}(P_l + P_{outcome})$. The mixture distribution helps with averaging and smoothing out the values, which causes the JSD to be bounded.

Although the JSD is bounded, in our approach, the upper bound depends on the number of layers in the network, causing problems in interpreting and comparing the results for networks with different numbers of layers. Therefore, we propose to normalize the UC results by dividing them by the upper bound of the UC metric. The upper bound of UC for a network with m layers (including the final teacher layer) can be computed as

$$UC_{max} = \sum_{l=1}^{m-1} W(l) \times \log_b(2), \quad (13)$$

where b is the logarithm base used to compute JSD. In our work, we are using the natural logarithm, i.e., $b = e$. $W(l)$ computes the weight at layer l . We can finally compute our normalized metric as

$$UC_{norm} = \frac{UC}{UC_{max}}. \quad (14)$$

Algorithm 1 outlines the steps to compute model uncertainty with our proposed disagreement metric. The algorithm relies on predictions from both the teacher and student models, as shown in line 2. If the student’s prediction differs from the outcome of the teacher/reference model, the weight function computes the classifier’s weight based on its depth (lines 3 to 12).

4 Experimental Evaluations

The proposed approach aims for precise and efficient GNN uncertainty quantification. We assess precision by comparing its uncertainty values with the dis-

Input: Graph input x , trained GNN M , and total number of layers m
Output: Uncertainty value u

```

1  $u \leftarrow 0$ 
2  $(preds_t, preds_s) \leftarrow M(x)$  // Step 1: Get predictions
3  $w \leftarrow [m]$  // Step 2: Compute weights (array of size  $m$ ).
4  $outcome\_class = \text{argmax}(preds_t)$ 
5 for  $l \leftarrow 1$  to  $(m - 1)$  do
6    $student\_class = \text{argmax}(preds_s[l])$ 
7   if  $student\_class \neq outcome\_class$  then
8      $w[l] \leftarrow 1 + \text{weight\_fn}(l, m)$ 
9   else
10     $w[l] \leftarrow 1$ 
11  end
12 end
13  $d \leftarrow [m]$  // Step 3: Compute disagreements (array of size  $m$ ).
14 for  $l \leftarrow 1$  to  $(m - 1)$  do
15    $d[l] \leftarrow \text{disagreement}(preds_s[l], preds_t)$ 
16 end
17  $u \leftarrow \text{sum}(w \times d)$  // Step 4: Compute uncertainty.
18 return  $u$ 

```

Algorithm 1: Quantifying the uncertainty of the GNN prediction

agreement metric in cases where there is a mismatch between the predictions of the reference and the shallow classifier. Efficiency is evaluated by comparing training and inference times against a single GNN, MC Dropout, and an independent ensemble. We also test OOD detection capabilities and measure potential classification performance overhead compared to the ensemble and MC Dropout.

4.1 Experimental Setup

Dataset: We used the publicly available MIMIC-IV dataset [12], containing medical data of over 200,000 patients labeled as "Not Readmitted," "Admitted to ICU," or "Admitted for Other Reasons" within 30 days of a hospital visit. For each patient, we constructed a heterogeneous directed graph with **visit nodes** (admission type, location) and **service nodes** (service code), following [4]. Edges connect temporally ordered visits and visits to utilized services. We used the "Admitted to ICU" as OOD data. For training, we balanced the "Not Admitted" (213,547 patients) and "Admitted for Other Reasons" (7,359 patients) groups by undersampling the former to 7,359 patients. To evaluate generalizability, we also utilized the Enzymes dataset [18], which comprises 600 graphs, each with an average of 32.6 nodes, each node having 18 features. The dataset contains six classes, where five classes are used for training and the last for OOD detection.

Models: For the Enzymes dataset, we utilized a graph classifier with four GraphSAGE [9] layers in all three approaches. The models follow the GNN structure provided by [5]. The ensemble approach trains four identical networks with different random initializations. The MC Dropout approach utilizes a dropout layer

before the fully connected layer, and the Self-Distillation approach adds a classifier after each GNN layer. For the MIMIC-IV dataset, we followed the same strategy as the Enzymes dataset, with the only difference being that the networks have three GraphConv [19] layers and there are three models in the ensemble. We followed the same structure and pooling layer suggested by [4].

Training and Hardware Specifications: All models were implemented using Python version 3.9 and PyTorch version 1.13.1. The models have been trained on a GPU (NVIDIA GeForce RTX 3050) with CUDA version 12.5. To optimize the networks, we used Adam Optimizer. We conducted a stratified 5-fold cross-validation. In each iteration, 80% of the training data was used for training, and the rest for validation. To aid the training process and prevent overfitting, batch normalization and dropout techniques were used for all models.

For comparison, ensemble and MC Dropout models were trained with Cross-Entropy Loss, while the self-distillation model used the loss in Equation 5. Consistent data folds and splits were used across methods. For self-distillation, we used $\alpha = 0.6$ and $\lambda = 0.04$, except for the reference layer, where we set α and λ to zero for the last 20 epochs to aid convergence as suggested in [24]. Limited hyperparameter tuning of α showed that 0.6 yielded lower mean uncertainty without complete teacher copying. We acknowledge that a more in-depth ablation study is necessary.

4.2 Results and Discussion

Table 2 shows the average performance, training time, inference time (in seconds), calibration errors on test data, and number of model parameters. For the Maximum Calibration Error (MCE), we used 10 bins. MC Dropout predictions were sampled 100 times, using the mean predicted probability for decisions. The models have not been calibrated, as shown by the similar calibration errors (MCE and Brier score). All approaches perform similarly on both datasets. However, the self-distillation approach has comparable training and inference times to those of a single model, thereby reducing the computational cost of using multiple GNN models, which is particularly important for resource-limited devices. On more complex graphs, such as MIMIC-IV, execution time increases for all methods; however, self-distillation retains an inference time comparable to that of a single model. Adding a harmonization layer before each classifier in self-distillation would slightly increase complexity, but as a shallow linear layer, the approach remains more efficient than the two baselines. Table 2 also shows that the ensemble has 3x (MIMIC-IV) and 4x (Enzymes) more parameters than single models. Self-distillation and MC Dropout have comparable parameters, making them more efficient to train and use. However, MC Dropout’s 100 inference samples make self-distillation more computationally efficient overall, especially for resource-constrained deployment, such as in heart-rate monitoring devices.

Finding 1: Using the proposed approach, we can efficiently train multiple GNN classifiers simultaneously, while achieving performance levels comparable to the

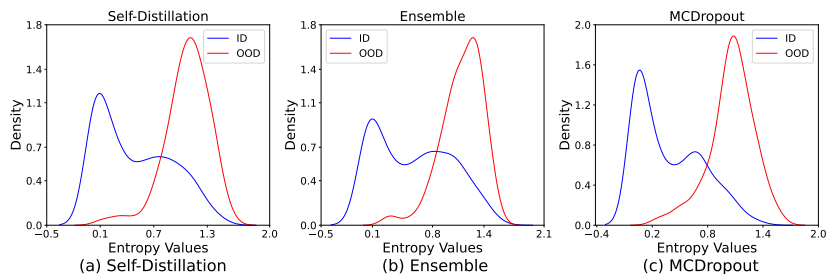


Fig. 2. KDE plots of entropy for self-distillation (a), ensembles (b), and MC Dropout (c) on Enzymes dataset. X-axis: entropy; Y-axis: probability density.

MCDropout method and an ensemble of GNNs.

We evaluated trained ensemble, self-distillation, and MC Dropout models on in-distribution (ID) and out-of-distribution (OOD) Enzymes data by comparing the entropy of their predictions (Figure 2). Higher entropy for OOD data (the red plot in Figure 2) indicates successful distinction across all methods. The Enzymes dataset’s six distinct classes made it suitable for visualizing this separation, unlike the less distinct classes in MIMIC-IV.

Self-distillation shows lower entropy on ID data than the ensemble, indicating lower uncertainty. The ensemble exhibits higher uncertainty even for ID data. This is because self-distillation trains shallower models to mimic a deeper reference model; close agreement suggests easily classified data with lower uncertainty. In contrast, independently trained ensemble members lead to higher entropy on ID data.

Finding 2: The proposed approach shows lower entropy on ID data but higher on OOD data, akin to the ensemble and MCDropout methods. The ensemble aims not to align models on class prediction, leading to slightly higher entropy on ID data than the proposed approach.

Table 3 shows two MIMIC-IV test cases. Patient 1 has unanimous "No Admission" predictions, while Patient 2 has complete disagreement. Consequently,

Table 2. Performance, train and inference time, calibration error, and number of parameters for each method.

Dataset	Model	F1-Score	ROC AUC	Train Time	Test Time	MCE	Brier	Params
MIMIC-IV	Single Model	0.83 ± 0.06	0.89 ± 0.0	293.10 ± 2.07	0.53 ± 0.07	-	-	142,978
	MC Dropout	0.85 ± 0.05	0.89 ± 0.01	319.18 ± 5.09	19.19 ± 0.17	0.11 ± 0.02	0.11 ± 0.01	142,978
	Ensemble	0.84 ± 0.07	0.89 ± 0.01	880.71 ± 6.92	1.48 ± 0.15	0.15 ± 0.06	0.12 ± 0.02	428,934
	Self-Distillation	0.88 ± 0.03	0.90 ± 0.0	320.04 ± 3.33	0.50 ± 0.02	0.14 ± 0.06	0.11 ± 0.01	144,006
Enzymes	Single Model	0.64 ± 0.04	0.85 ± 0.03	51.67 ± 2.16	0.02 ± 0.0	-	-	73,082
	MC Dropout	0.66 ± 0.03	0.88 ± 0.02	40.92 ± 1.94	1.24 ± 0.06	0.46 ± 0.08	0.53 ± 0.05	73,082
	Ensemble	0.68 ± 0.03	0.89 ± 0.02	204.29 ± 4.01	0.08 ± 0.0	0.40 ± 0.12	0.44 ± 0.05	292,328
	Self-Distillation	0.67 ± 0.02	0.87 ± 0.02	91.78 ± 2.36	0.02 ± 0.0	0.42 ± 0.10	0.51 ± 0.04	88,748

Table 4 demonstrates higher uncertainty for Patient 2 using the proposed metrics, Equations 11 and 14, despite equal disagreement using Equation 6, are highlighting the metric’s sensitivity to prediction diversity of diverse classifiers.

The disagreement metric in Equation 6 fails to capture varying difficulty levels between samples, as shown in Table 4. While both patients have the same disagreement value, Patient 2’s classifiers show a disagreement in the predicted class from the reference, indicating greater difficulty. Our proposed uncertainty metric addresses this by assigning higher disagreement values for more challenging cases. Both patients were correctly classified by the reference classifier. Furthermore, Patient 2’s misclassification, unlike Patient 1’s correct classification by the shallower classifiers, highlights the need for precise uncertainty metrics in healthcare to improve clinician trust and decision-making. This is especially challenging when deep learning models need to be deployed on edge devices, such as wearable heart-rate monitoring systems with limited computational resources.

Table 3. Disagreement between reference and shallower classifiers for two MIMIC-IV patients.

Model	Patient 1		Patient 2	
	No ADT	ADT	No ADT	ADT
Classifier 1	<i>87.89</i>	12.11	<i>57.91</i>	42.09
Classifier 2	<i>99.14</i>	0.86	<i>68.16</i>	31.84
Ref. Classifier	<i>97.53</i>	2.47	47.54	<i>52.46</i>

Table 4. MIMIC-IV sample scenario illustrating the agreement metric’s lack of expressivity.

Metrics	Patient 1	Patient 2
Disagreement	0.1082	0.1082
UC (Linear Weight)	0.0207	0.0438
UC (Nonlinear Weight)	0.0207	0.0498
UC _{norm} (Linear Weight)	0.0099	0.0211
UC _{norm} (Nonlinear Weight)	0.0085	0.0205

Finding 3: The uncertainty quantification metric distinguishes scenarios with discrepancies between the teacher classifier’s predicted label and shallower classifiers, making it more precise than the earlier disagreement metric.

5 Conclusion

This paper presents an efficient and precise method to quantify predictive uncertainty in GNNs. We use self-distillation to train diverse teacher-student models in a single training process. Our approach utilizes the Jensen-Shannon divergence and a weight function to assess uncertainty, capturing disagreement between the student and teacher models. The evaluation shows performance comparable to that of the ensemble and MC Dropout methods, with reduced training and inference time. Additionally, the method identifies scenarios where student predictions diverge from a reference model.

As a future direction, we plan to explore alternative teacher selection methods (e.g., ensemble teacher distillation, transitive teacher distillation, and dense teacher distillation) [24] to confirm that our proposed technique for quantifying uncertainty can be applied to different self-distillation strategies. Furthermore, we aim to carry out a more thorough analysis of the weight function selection

to investigate the impact of different weight functions on uncertainty quantification. Additionally, we will develop interpretable uncertainty values to improve clinical decision-making. Finally, we plan to conduct a more in-depth ablation study to investigate the impact of different values for imitation (α) and trade-off (λ) parameters in the training of student models.

Acknowledgments. This study is supported by the *Pediatric Mental Health Learning Health System* research project and funded by the *Hamilton Health Sciences RFA Research Strategic Initiative Program* and *Natural Sciences and Engineering Research Council of Canada (NSERC) Discovery* grants. This research was also undertaken thanks in part to funding from the *Canada First Research Excellence Fund*. We would like to extend our deepest gratitude to Dr. Roberto Sassi (Associate Professor and Division Head, Child & Adolescent Psychiatry, University of British Columbia), Dr. Paulo Pires (Psychologist and Clinical Director for the CYMHP) and Dr. Laura Duncan (Assistant Professor, Psychiatry & Behavioural Neurosciences, McMaster University), for their valuable insights.

Disclosure of Interests. The authors have no competing interests to declare that are relevant to the content of this article.

References

1. Aouichaoui, A.R.N., Mansouri, S.S., Abildskov, J., Sin, G.: Uncertainty estimation in deep learning-based property models: Graph neural networks applied to the critical properties. *AIChE Journal* **68**(6), e17696 (2022). <https://doi.org/https://doi.org/10.1002/aic.17696>
2. Chen, Y., Bian, Y., Xiao, X., Rong, Y., Xu, T., Huang, J.: On self-distilling graph neural network (2021), <https://arxiv.org/abs/2011.02255>
3. Daneshvar, H., Boursalie, O., Samavi, R., Doyle, T.E., Duncan, L., Pires, P., Sassi, R.: Sok: Application of machine learning models in child and youth mental health decision-making. *Artificial Intelligence for Medicine* pp. 113–132 (2024). <https://doi.org/10.1016/B978-0-443-13671-9.00003-X>
4. Daneshvar, H., Samavi, R.: Heterogeneous Patient Graph Embedding in Readmission Prediction. *Proceedings of the Canadian Conference on Artificial Intelligence* (may 27 2022). <https://doi.org/10.21428/594757db.869abbde>
5. Dwivedi, V.P., Joshi, C.K., Luu, A.T., Laurent, T., Bengio, Y., Bresson, X.: Benchmarking graph neural networks. *Journal of Machine Learning Research* **24**(43), 1–48 (2023), <http://jmlr.org/papers/v24/22-0567.html>
6. Gheshlaghi, S.H., Soltani, N.Y., Ganji, M.: Uncertainty estimation for out-of-distribution detection of whole slide images. In: *ICASSP 2025 - 2025 IEEE International Conference on Acoustics, Speech and Signal Processing (ICASSP)*. pp. 1–5 (2025). <https://doi.org/10.1109/ICASSP49660.2025.10889349>
7. Gou, J., Yu, B., Maybank, S.J., Tao, D.: Knowledge distillation: A survey. *International Journal of Computer Vision* **129**(6), 1789–1819 (Jun 2021). <https://doi.org/10.1007/s11263-021-01453-z>
8. H. Zargarbashi, S., Antonelli, S., Bojchevski, A.: Conformal prediction sets for graph neural networks. In: Krause, A., Brunskill, E., Cho, K., Engelhardt, B., Sabato, S., Scarlett, J. (eds.) *Proceedings of the 40th International Conference on*

- Machine Learning. Proceedings of Machine Learning Research, vol. 202, pp. 12292–12318. PMLR (07 2023), <https://proceedings.mlr.press/v202/h-zargarbashi23a.html>
9. Hamilton, W., Ying, Z., Leskovec, J.: Inductive representation learning on large graphs. In: Guyon, I., Luxburg, U.V., Bengio, S., Wallach, H., Fergus, R., Vishwanathan, S., Garnett, R. (eds.) Advances in Neural Information Processing Systems. vol. 30. Curran Associates, Inc. (2017), https://proceedings.neurips.cc/paper_files/paper/2017/file/5dd9db5e033da9c6fb5ba83c7a7ebea9-Paper.pdf
 10. Hinton, G., Vinyals, O., Dean, J.: Distilling the knowledge in a neural network (2015), <https://arxiv.org/abs/1503.02531>
 11. Huang, K., Jin, Y., Candes, E., Leskovec, J.: Uncertainty quantification over graph with conformalized graph neural networks. In: Oh, A., Naumann, T., Globerson, A., Saenko, K., Hardt, M., Levine, S. (eds.) Advances in Neural Information Processing Systems. vol. 36, pp. 26699–26721. Curran Associates, Inc. (2023), https://proceedings.neurips.cc/paper_files/paper/2023/file/54a1495b06c4ee2f07184afb9a37abda-Paper-Conference.pdf
 12. Johnson, A., Bulgarelli, L., Pollard, T., Gow, B., Moody, B., Horng, S., Celi, L.A., Mark, R.: MIMIC-IV (2024)
 13. Karimi, H., Samavi, R.: Quantifying deep learning model uncertainty in conformal prediction. In: Proceedings of the AAAI Symposium Series. vol. 1, pp. 142–148 (2023)
 14. Karimi, H., Samavi, R.: Evidential uncertainty sets in deep classifiers using conformal prediction. In: Proceedings of the Thirteenth Symposium on Conformal and Probabilistic Prediction with Applications, PMLR. vol. 230, pp. 466–489 (2024)
 15. Kwon, Y., Lee, D., Choi, Y.S., Kang, S.: Uncertainty-aware prediction of chemical reaction yields with graph neural networks. *Journal of Cheminformatics* **14**(1), 2 (1 2022). <https://doi.org/10.1186/s13321-021-00579-z>
 16. Lakshminarayanan, B., Pritzel, A., Blundell, C.: Simple and scalable predictive uncertainty estimation using deep ensembles. In: Guyon, I., Luxburg, U.V., Bengio, S., Wallach, H., Fergus, R., Vishwanathan, S., Garnett, R. (eds.) Advances in Neural Information Processing Systems. vol. 30. Curran Associates, Inc. (2017), https://proceedings.neurips.cc/paper_files/paper/2017/file/9ef2ed4b7fd2c810847ffa5fa85bce38-Paper.pdf
 17. Liu, Z., Li, X., Peng, H., He, L., Philip, S.Y.: Heterogeneous Similarity Graph Neural Network on Electronic Health Records. In: 2020 IEEE International Conference on Big Data (Big Data). pp. 1196–1205. IEEE (2020)
 18. Morris, C., Kriege, N.M., Bause, F., Kersting, K., Mutzel, P., Neumann, M.: TUDataset: A collection of benchmark datasets for learning with graphs. In: ICML 2020 Workshop on Graph Representation Learning and Beyond (GRL+ 2020) (2020), www.graphlearning.io
 19. Morris, C., Ritzert, M., Fey, M., Hamilton, W.L., Lenssen, J.E., Rattan, G., Grohe, M.: Weisfeiler and Leman Go Neural: Higher-order Graph Neural Networks (2021)
 20. Phuong, M., Lampert, C.: Towards understanding knowledge distillation. In: Chaudhuri, K., Salakhutdinov, R. (eds.) Proceedings of the 36th International Conference on Machine Learning. Proceedings of Machine Learning Research, vol. 97, pp. 5142–5151. PMLR (09–15 Jun 2019), <https://proceedings.mlr.press/v97/phuong19a.html>
 21. Shang, J., Ma, T., Xiao, C., Sun, J.: Pre-training of Graph Augmented Transformers for Medication Recommendation (2019)
 22. Vovk, V., Gammerman, A., Shafer, G.: Algorithmic learning in a random world, vol. 29. Springer (2005)

23. Wang, F., Liu, Y., Liu, K., Wang, Y., Medya, S., Yu, P.S.: Uncertainty in graph neural networks: A survey (2024), <https://arxiv.org/abs/2403.07185>
24. Zhang, L., Bao, C., Ma, K.: Self-distillation: Towards efficient and compact neural networks. *IEEE Transactions on Pattern Analysis and Machine Intelligence* **44**(8), 4388–4403 (2022). <https://doi.org/10.1109/TPAMI.2021.3067100>
25. Zhang, W., Miao, X., Shao, Y., Jiang, J., Chen, L., Ruas, O., Cui, B.: Reliable data distillation on graph convolutional network. In: *Proceedings of the 2020 ACM SIGMOD International Conference on Management of Data*. p. 1399–1414. SIGMOD '20, Association for Computing Machinery, New York, NY, USA (2020). <https://doi.org/10.1145/3318464.3389706>
26. Zhang, Y., Lee, A.A.: Bayesian semi-supervised learning for uncertainty-calibrated prediction of molecular properties and active learning. *Chem. Sci.* **10**, 8154–8163 (2019). <https://doi.org/10.1039/C9SC00616H>
27. Zhu, W., Razavian, N.: Variationally Regularized Graph-Based Representation Learning for Electronic Health Records. In: *Proceedings of the Conference on Health, Inference, and Learning*. pp. 1–13. CHIL '21, Association for Computing Machinery, New York, NY, USA (2021). <https://doi.org/10.1145/3450439.3451855>, <https://doi.org/10.1145/3450439.3451855>